

A bivalent cyclic RGD–siRNA conjugate enhances the antitumor effect of apatinib via co-inhibiting VEGFR2 in non-small cell lung cancer xenografts

Lumin Liao^a, Bohong Cen^{b,c}, Guoxian Li^a, Yuanyi Wei^b, Zhen Wang^b, Wen Huang^b, Shuai He^{b*}, Yawei Yuan^c and Aimin Ji^a

^aDepartment of Pharmacy, The Seventh Affiliated Hospital, Southern Medical University, Foshan, Guangdong, China; ^bDepartment of Pharmacy, Zhujiang Hospital, Southern Medical University, Guangzhou, Guangdong, China; ^cDepartment of Radiation Oncology, Affiliated Cancer Hospital & Institute of Guangzhou Medical University, Guangzhou, Guangdong, China

ABSTRACT

The vascular endothelial growth factor receptor 2 (VEGFR2) is considered to be a pivotal target for anti-tumor therapy against angiogenesis of non-small cell lung cancer (NSCLC). However, effective and low-toxicity targeted therapies to inhibit VEGFR2 are still lacking. Here, biRGD–siVEGFR2 conjugate comprising murine VEGFR2 siRNA and [cyclo(Arg-Gly-Asp-D-Phe-Lys)-Ahx]₂-Glu-PEG-MAL (biRGD) peptide which selectively binds to integrin $\alpha v \beta 3$ receptors expressing on neovascularization endothelial cell was synthesized. The anti-tumor activity and renal toxicity of biRGD–siVEGFR2 or its combination therapy with low-dose apatinib were investigated on NSCLC xenografts. The immunogenicity of biRGD–siVEGFR2 was also evaluated in C57BL/6J mice. *In vivo*, intravenously injected biRGD–siVEGFR2 substantially inhibited NSCLC growth with a marked reduction of vessels and a down-regulation of VEGFR2 in tumor tissue. Furthermore, biRGD–siVEGFR2 in combination with low-dose apatinib achieved powerful anti-tumor effect with less nephrotoxicity compared with the regular dose of apatinib. Besides, no obvious immunogenicity of biRGD–siVEGFR2 was found. These findings demonstrate that biRGD–siVEGFR2 conjugate can be used as a new candidate for the treatment of NSCLC and its combination therapy with apatinib may also provide a novel strategy for cancer treatment in clinic.

ARTICLE HISTORY

Received 10 April 2021
Revised 23 May 2021
Accepted 25 May 2021

KEYWORDS

siRNA delivery; VEGFR2; angiogenesis; combination therapy; non-small cell lung cancer (NSCLC)







1. Introduction


Non-small cell lung cancer (NSCLC) is the most common human malignancy in the world with increasing morbidity and mortality every year (Bray et al., 2018). Angiogenesis is an indispensable factor for NSCLC progression (Manzo et al., 2017). Currently, antiangiogenic therapy has been added to the standard treatment for patients with NSCLC (Hall et al., 2015). The vascular endothelial growth factor receptor 2 (VEGFR2, also known as KDR/Flk-1) plays a critical role in angiogenic process, during which VEGF binds to VEGFR2, then activates downstream angiogenic signaling pathways and results in proliferation and migration of endothelial vessels, consequently promoting angiogenesis and tumor proliferation (Carmeliet & Jain, 2011; Piperdi et al., 2014). Therefore, inhibition of VEGFR2 in neovascularization is an effective method for antiangiogenic therapy in NSCLC.

Apatinib, also known as YN968D1, is a novel oral tyrosine kinase inhibitor (TKI) that selectively inhibits VEGFR2, thus exerting an antiangiogenic effect and inhibiting tumor

proliferation including NSCLC (Tian et al., 2011; Fan et al., 2020). Especially, apatinib has showed several notable characteristics, such as promoting tumor size shrinkage, inducing tumor regression and facilitating metastasis confinement, which are rarely found in other anti-angiogenic drugs. However, apatinib is also faced with the dilemma of short term of response, drug resistance and adverse effects including hypertension, proteinuria and hand-foot syndrome when it is used for a long time (Yang et al., 2020). Therefore, it is necessary to develop new targeted therapy to inhibit VEGFR2 in order to obtain better anti-tumor activity, fewer side effects and lower drug resistance.

RNA interference (RNAi) is a post-transcriptional gene regulatory process triggered by small interfering RNAs (siRNAs), which has the potential to treat tumor via silencing any disease-related genes in a sequence-specific manner (Barata et al., 2016; Shen et al., 2018). After a 20-year journey from its discovery, the United States Food and Drug Administration (FDA) and European Commission (EC) approved ONPATTRO[®] (patisiran, ALN-TTR02) achieved by

CONTACT Aimin Ji  aiminji_007@163.com  Department of Pharmacy, The Seventh Affiliated Hospital, Southern Medical University, Foshan 528244, Guangdong, China; Yawei Yuan  yuanyawei@gzhu.edu.cn  Department of Radiation Oncology, Affiliated Cancer Hospital & Institute of Guangzhou Medical University, Guangzhou 510095, Guangdong, China; Shuai He  hs43555@163.com  Department of Pharmacy, Zhujiang Hospital, Southern Medical University, Guangzhou 510280, Guangdong, China

 Supplemental data for this article can be accessed [here](#).

*Key Laboratory of New Drug Screening, Zhujiang Hospital, Southern Medical University, Guangzhou 510280, Guangdong, China.

© 2021 The Author(s). Published by Informa UK Limited, trading as Taylor & Francis Group.

This is an Open Access article distributed under the terms of the Creative Commons Attribution-NonCommercial License (<http://creativecommons.org/licenses/by-nc/4.0/>), which permits unrestricted non-commercial use, distribution, and reproduction in any medium, provided the original work is properly cited.

Alnylam Pharmaceuticals (Cambridge, MA) as the first commercial siRNA therapeutic agent for the treatment of hereditary transthyretin amyloidosis (hATTR) with polyneuropathy in adults in 2018, which officially declared that RNAi therapy has come from theory to reality (Ruger et al., 2020). siRNA has innate advantages over small molecular therapeutics because siRNA executes its function by complete base pairing with mRNA, whereas small molecule drugs need to recognize the complicated spatial conformation of certain proteins, which confers the siRNA therapy with a shorter research and development span and a wider therapeutic area than small molecule drugs (Hu et al., 2020).

Even though siRNA technology has shown promising prospects in both preclinical and clinical trials, several barriers limit its clinical application (Ozcan et al., 2015). Intravenously injected siRNA is rapidly cleared without being taken up by target cells because it is a negatively charged macromolecule that has no bioavailability to cross cell membranes (Wittrup & Lieberman, 2015). Therefore, various chemically modified geometries and delivery systems such as nanoparticles and conjugates were established to assist the delivery of siRNA (Shen et al., 2017; Caillaud et al., 2020). Although nano-delivery systems show powerful delivery capabilities, they still have certain unavoidable disadvantages, such as burst release, toxicity risk associated with cationic materials and fast uptake by MPS cells (Caillaud et al., 2020). As an alternative to nano-delivery systems, researchers searched for a novel way to deliver siRNA. They obtained siRNA conjugates by directly linking siRNA covalently to different bioactive groups, such as lipids, aptamers and carbohydrates, which have been studied in preclinical and clinical trials (Lee et al., 2016; Weng et al., 2019). For example, GIVLAARI[®] (givosiran) from Alnylam (Cambridge, MA), a conjugate of N-acetylgalactosamine (GalNAc) to siRNA which enables specific binding to asialoglycoprotein receptor on hepatocytes, is approved to treat acute hepatic porphyria (AHP) in adults by FDA (Debacker et al., 2020). Currently, seven GalNAc-siRNA conjugates from Alnylam (Cambridge, MA) are undergoing clinical trials for liver genes, which show satisfactory progress (Hu et al., 2020). Similarly, in this study, we prepared a biRGD-siRNA conjugate by linking siRNA to the bivalent [cyclo(Arg-Gly-Asp-D-Phe-Lys)-Ahx]₂-Glu-PEG-MAL peptide as our previous study shown (Cen et al., 2018).

Integrin $\alpha\beta 3$ receptors which play a key role in angiogenesis and tumor metastasis are significantly up-regulated in tumor neovascular endothelial cells and certain solid tumors such as glioblastoma, but not in quiescent endothelial cells and normal tissues (Beer & Schwaiger, 2008; Alday-Parejo et al., 2019). Several studies have confirmed that the arginine-glycine-aspartate peptide (RGD) can be specifically recognized by $\alpha\beta 3$ receptors and carry molecules into cells via $\alpha\beta 3$ receptor-mediated endocytosis (Liu et al., 2014a,b; Arosio & Casagrande, 2016; He et al., 2017; Cen et al., 2018). As of August 2020, more than 50 clinical trials of RGD-based tumor tracers or tumor-targeted drugs have been registered in the US FDA Clinical Trial Center. Therefore, RGD-based delivery systems have the potential to treat tumors.

This study intended to construct biRGD-siVEGFR2 conjugate delivery system which can silence VEGFR2 expression with targeting to neovascularization endothelial cells. Then we established an NSCLC model to observe the antitumor efficacy and renal toxicity of biRGD-siVEGFR2 monotherapy and its combination therapy with apatinib. Furthermore, we also evaluated the immunogenicity of biRGD-siVEGFR2 in C57BL/6J mice with intact immune system. To our knowledge, this is the first study to evaluate the antitumor activity of combination therapy with siRNA conjugate and small molecule TKI via co-inhibiting VEGFR2 gene.

2. Materials and methods

2.1. Cell culture

The luciferase-expressed A549 cell line (human non-small cell lung cancer cell line) was kindly provided by Guangzhou RiboBio Co., Ltd. (Guangzhou, China). MS1 cell line (the mouse islet endothelial cell line, Catalog No. CRL-2279) was purchased from ATCC (Manassas, VA). Cells were cultured using supplier recommended reagents and grown at 37 °C in a humidified atmosphere of 5% CO₂ according to standard protocols and procedures.

2.2. Synthesis of biRGD-siRNA

In the preparation of biRGD-siRNA molecules, two 6-aminocaproic acids, one glutamic acid and two cRGD moieties underwent intermolecular dehydration condensation to form biRGD structure, which was covalently coupled to the 5' end of siRNA sense strand via thiol-maleimide linker. The specific synthetic process and validation were performed as our previous description (Cen et al., 2018). The targeted murine VEGFR2 siRNA (siVEGFR2) and negative control siRNA (siNC) were synthesized by Guangzhou RiboBio Co., Ltd. (Guangzhou, China). Murine siVEGFR2 sequence refers to previous studies (Chen et al., 2013; Liu et al., 2014b). The details of siRNA sequences and modifications for this experiment were siVEGFR2 (sense strand: 5'-(mC)G(mG)AGAAGAAUGUGGU(mU)A(mA)dTdT-3'; anti-sense strand: 5'-(mU)(mU)AACCACAUUCU(mU)C(mU)C(mC)GdTdT-3') and siNC (sense strand: 5'-(mC)(mG)(mU)GAUUGCGAGACUC(mU)(mG)(mA)dTdT-3'; anti-sense strand: 5'-(mU)(mC)(mA)GAGUCUCGCAUUC(mA)(mC)(mG)dTdT-3'). mN represented 2'-O-methyl (2'-OMe) sugar-modified RNA nucleosides.

2.3. Transfection experiments

Due to the lack of murine cell line with highly expressed integrin $\alpha\beta 3$, we delivered biRGD-siVEGFR2 to MS1 cells, commonly used to study angiogenic signal transduction, with lipofectamine 3000 (Invitrogen, Carlsbad, CA). The cells were harvested for RT-qPCR and western blot analysis after being transfected for 48 hours and 72 hours, respectively.

2.4. RT-qPCR

Total RNA was extracted from MS1 cells or tumor samples using RNAiso Plus reagent (TaKaRa, Maebashi, Japan) and reverse transcribed into cDNA using PrimeScript™ RT Reagent Kit with gDNA Eraser (TaKaRa, Maebashi, Japan) following the manufacturer's protocol. Real-time monitoring of the PCR amplification of the cDNA was performed using the Applied Biosystems 7500 real-time PCR system (Life Technologies, Carlsbad, CA) with SYBR® Premix Ex Taq™ Kit (TaKaRa, Maebashi, Japan). qPCR amplification was conducted following the manufacturer's protocol. Data were calculated using the $2^{-\Delta\Delta C_t}$ method. The primers sequences were GAPDH (forward (5'-3'): GGCATTGCTCTCAATGACAA; reverse (5'-3'): TGTGAGGGAGATGCTCAGTG) and VEGFR2 (forward (5'-3'): GCCAATGAAGGGGAAGACTGAAGAC; reverse (5'-3'): TCTGGCTGCTGGTGATGCTGTC).

2.5. Western blot

Total protein was extracted from MS1 cells or tumor samples, subjected to electrophoresis in 8% polyacrylamide gel and transferred to a polyvinylidene fluoride membrane (Millipore Corporation, Billerica, MA). The bands were blocked in 5% BSA for two hours at room temperature. After washing for three times with Tris-buffered saline containing 0.1% Tween 20 (TBST) every 10 minutes, the membranes were incubated with primary anti-mouse VEGFR2 antibody (Cell Signaling Technology, Boston, MA) and β -actin antibody (Proteintech Group, Rosemont, IL) at 4°C overnight. As described above, the membranes were washed and incubated with goat anti-rabbit secondary antibody (Proteintech Group, Rosemont, IL) for two hours and detected with ECL Chemiluminescence Substrate Reagent (Millipore Corporation, Billerica, MA) according to the manufacturer's instructions. The densities of bands were scanned and calculated by Image J software (Bethesda, MD).

2.6. Animal handling

C57BL/6J mice (female, 4–6 weeks, ~20 g) and BALB/c nude mice (female, 4–6 weeks, ~20 g) were purchased from the Experimental Animal Center of Sun Yat-sen University (Guangzhou, China) and raised in a specific-pathogen-free environment according to standardized animal care guidelines. The experiments were approved by the Southern Medical University animal experiments ethical committee and carried out according to national regulations.

2.7. Anti-tumor activity

BALB/c nude mice were subcutaneously inoculated with 6×10^6 luciferase-A549 cells to establish human NSCLC tumor model. When tumor volume reached 50–60 mm³, all tumor-bearing mice were randomly divided into six groups (n = 5). Saline group; biRGD-siNC (2 nmol/20 g) group; biRGD-siVEGFR2 (1 nmol/20 g) group; biRGD-siVEGFR2 (2 mol/20 g) group; apatinib (2.6 mg/20 g) group;

biRGD-siVEGFR2 (1 nmol/20 g)+apatinib (1.3 mg/20 g) combination group. Tumor-bearing mice were intravenously injected with biRGD-siVEGFR2 for seven times with an interval of 48 hours between each injection or given apatinib intragastrically in the same interval. Tumor diameter was measured by a vernier caliper before each treatment and the volume was calculated using the formula: Volume = $1/2 \times \text{Length} \times (\text{Width})^2$. Besides, tumor growth was also monitored by intratumoral fluorescence intensity via an *in vivo* imaging system (IVIS Lumina II, Caliper, Hopkinton, MA) on day 0, 5, 10 and 15 after treatment.

To further investigate whether biRGD-siVEGFR2 was dose-dependent, we reestablished a NSCLC xenograft tumor model as described above, increased the dose of biRGD-siVEGFR2 and compared its anti-tumor efficiency with that of apatinib. The apatinib-treated mice were administered at a dose of 2.6 mg/20 g body weight, which was converted from clinically regular dose. At the same time, a combination group containing biRGD-siVEGFR2 and gelofusine was added to alleviate the possible tubulointerstitial injury caused by high dose of biRGD-siRNA mentioned in our previous study (He et al., 2017; Cen et al., 2018). All the tumor-bearing mice were randomly divided into five groups (n = 5), when the tumor volume reached 100–150 mm³. Saline group; biRGD-siNC (5 nmol/20 g) group; biRGD-siVEGFR2 (5 nmol/20 g) group; biRGD-siVEGFR2 (5 nmol/20 g)+gelofusine (4 mg/20 g) group; apatinib (2.6 mg/20 g) group. Assays and analytical methods were the same as described above except for the different dosing regimen.

2.8. Immunohistochemistry analysis

Tumors isolated from all experimental groups were fixed immediately with 4% paraformaldehyde, embedded in paraffin and then cut into 4 μ m thick sections. Primary antibodies including anti-CD31 antibody (catalog number: AF3628) from R&D Systems (Minneapolis, MN) and anti-Ki67 antibody (catalog number: ARG53222) from Arigo Biolaboratories (Shanghai, China) were used to label the positive expression of CD31 and Ki67 in tumor tissues in order to observe microvessel density and tumor cells proliferation.

2.9. Toxicity evaluation in vivo

Three days after the last administration, serum was collected from tumor-bearing mice. Aspartate aminotransferase (AST), alanine aminotransferase (ALT), creatinine (Cr) and urea nitrogen (BUN) were detected by automatic Aeroset Chemistry Analyzer (Abbott, Abbott Park, IL) following the manufacturer's instructions.

As described above, the kidneys were isolated, embedded and sectioned. All sections were stained with hematoxylin-eosin for histological examination according to standard clinical laboratory procedures.

2.10. Immunogenicity evaluation of biRGD–siVEGFR2 *in vivo*

C57BL/6J mice were randomly divided into saline group ($n=5$) and biRGD–siVEGFR2 group (2 nmol/20 g, $n=5$). Six hours after the administration, blood was collected and serum was separated to measure the levels of cytokines IFN- α , IFN- β , IL-6 and IL-12 using ELISA Kit (Bio-Swamp, Wuhan, China) according to manufacturer's instructions.

2.11. Statistical analysis

All data were expressed as mean \pm standard deviation (SD) and statistical analysis was performed using SPSS 20.0 statistical software (Chicago, IL). Independent-samples *t*-test was used to compare two groups. One-way analysis of variance (ANOVA) was used for multiple comparison. $P < 0.05$ (two-tailed) was considered statistically significant different.

3. Results

3.1. Preparation and gene silencing efficiency of biRGD–siVEGFR2 *in vitro*

The diagram of biRGD–siVEGFR2 conjugate is shown in Figure 1(A). The double-stranded siVEGFR2 (sense strand: 5'-(mC)G(mG)AGAAGAAUGUGGU(mU)A(mA)dTdT-3'; anti-sense strand: 5'-(mU)(mU)AACCACAUUCU(mU)C(mU)C(mC)GdTdT-3') was selected as the representative siRNA drug, which was modified with 2'-OMe in recommended nucleotides so as to increase the stability and silencing potency and reduce the off-target effect and cytotoxicity. Here, the 5'-phosphate of sense strand of siVEGFR2 was linked to ((cyclo(Arg-Gly-Asp-D-Phe-Lys)-Ahx)₂-Glu-PEG-MAL) peptide through the thiol-maleimide linker, as shown in our previous report (Cen et al., 2018).

The RP-HPLC results revealed that the purity of biRGD–siVEGFR2 sense strand and antisense strand were both $>70\%$, as shown in Figure 1(B,D). HPLC–MS results showed that the molecular mass of biRGD–siVEGFR2 sense strand was 8890.6 Da acceptably close to the predicted mass of 8891.8 Da and the molecular mass of biRGD–siVEGFR2 antisense strand was 6559.9 Da acceptably close to the predicted mass of 6558.1 Da (Figure 1(C,E)), which indicated that the molecular mass of synthesized biRGD–siVEGFR2 was consistent with its theoretical molecular mass.

To validate the silencing efficiency of 2'-OMe-modified siVEGFR2 sequence in the biRGD conjugate, we transfected biRGD–siRNA into MS1 cells with lipofectamine 3000 due to the lack of mouse-derived neovascularization endothelial cell line with highly expression of $\alpha v\beta 3$ receptors. RT-qPCR analysis demonstrated that the VEGFR2 mRNA expression in MS1 cells transfected with 100 nM biRGD–siVEGFR2 was significantly decreased compared with that in the control group (the expression level was 42.68%, Figure S1A). Furthermore, western blot analysis showed that the VEGFR2 protein expression was also significantly decreased after treatment with 100 nM biRGD–siVEGFR2 for 72 hours compared with that in the parallel control group (the expression level was

29.33%, Figure S1B and S1C). In general, these data suggested that biRGD–siVEGFR2 was able to efficiently inhibit targeted gene expression.

3.2. Anti-non-small cell lung cancer activity of biRGD–siVEGFR2 and its combination with apatinib *in vivo*

A human NSCLC (A549-luc) xenograft expressing a luciferase reporter gene was established to investigate anti-tumor activity of biRGD–siVEGFR2 and its combination with apatinib *in vivo*. Briefly, nude mice bearing A549-Luc tumors were intravenously injected with biRGD–siVEGFR2 seven times over a 48 hours interval or given apatinib intragastrically in the same interval. The intratumoral fluorescence was visualized by bioimaging in Figure 2(A) and luciferase signal intensity was quantified and normalized in Figure 2(B).

As seen in Figure 2(A–D), these results demonstrated that all biRGD–siVEGFR2 treatment groups and apatinib groups significantly inhibited tumor growth after treating 15 days. Besides, the anti-tumor effects of biRGD–siVEGFR2 (1 nmol/20 g)/Apatinib (1.3 mg/20 g) combination group and high-dose apatinib (2.6 mg/20 g) group were more stronger than that of other groups, but there was no significant difference between biRGD–siVEGFR2 (1 nmol/20 g)/apatinib (1.3 mg/20 g) combination group and high-dose apatinib (2.6 mg/20 g) group.

More specifically, no significant difference was observed between saline and biRGD–siNC (2 nmol/20 g) groups, which indicated that biRGD–siNC did not have anti-tumor activity. Furthermore, on the fourth day after the first administration, compared with saline group, only biRGD–siVEGFR2 combination treatment group and apatinib (2.6 mg/20 g) group significantly inhibited tumor growth ($P < 0.05$) and there was no significant difference between these two groups ($P > 0.05$). Fifteen days after treatment, significant tumor growth inhibitions were observed in biRGD–siVEGFR2 (1 nmol/20 g), biRGD–siVEGFR2 (2 nmol/20 g), biRGD–siVEGFR2 (1 nmol/20 g)/apatinib (1.3 mg/20 g) combination group and apatinib (2.6 mg/20 g) alone group compared with that of saline and biRGD–siNC (2 nmol/20 g) administered groups ($P < 0.05$). The order of their effects was as follows: biRGD–siVEGFR2 (1 nmol/20 g)/apatinib (1.3 mg/20 g) combination group \approx apatinib (2.6 mg/20 g) alone group $>$ biRGD–siVEGFR2 (2 nmol/20 g) $>$ biRGD–siVEGFR2 (1 nmol/20 g).

These results suggested that biRGD–siVEGFR2 had the potential as an anti-NSCLC agent and tail vein injection at a dose higher than 1 nmol/20 g/48 h can effectively inhibit tumor growth. At the same time, biRGD–siVEGFR2 in combination with low-dose apatinib can achieve the same antitumor effect as the regular dose of apatinib. It is suggested that biRGD–siVEGFR2 can be used as an effective supplement for apatinib in clinical application.

Three days after the last injection, mice were euthanized and tumors were collected for further analysis. RT-qPCR and western blot results showed an obviously low expression of VEGFR2 mRNA and protein in all treatment groups compared with that in saline group (Figure 2(E,F)).

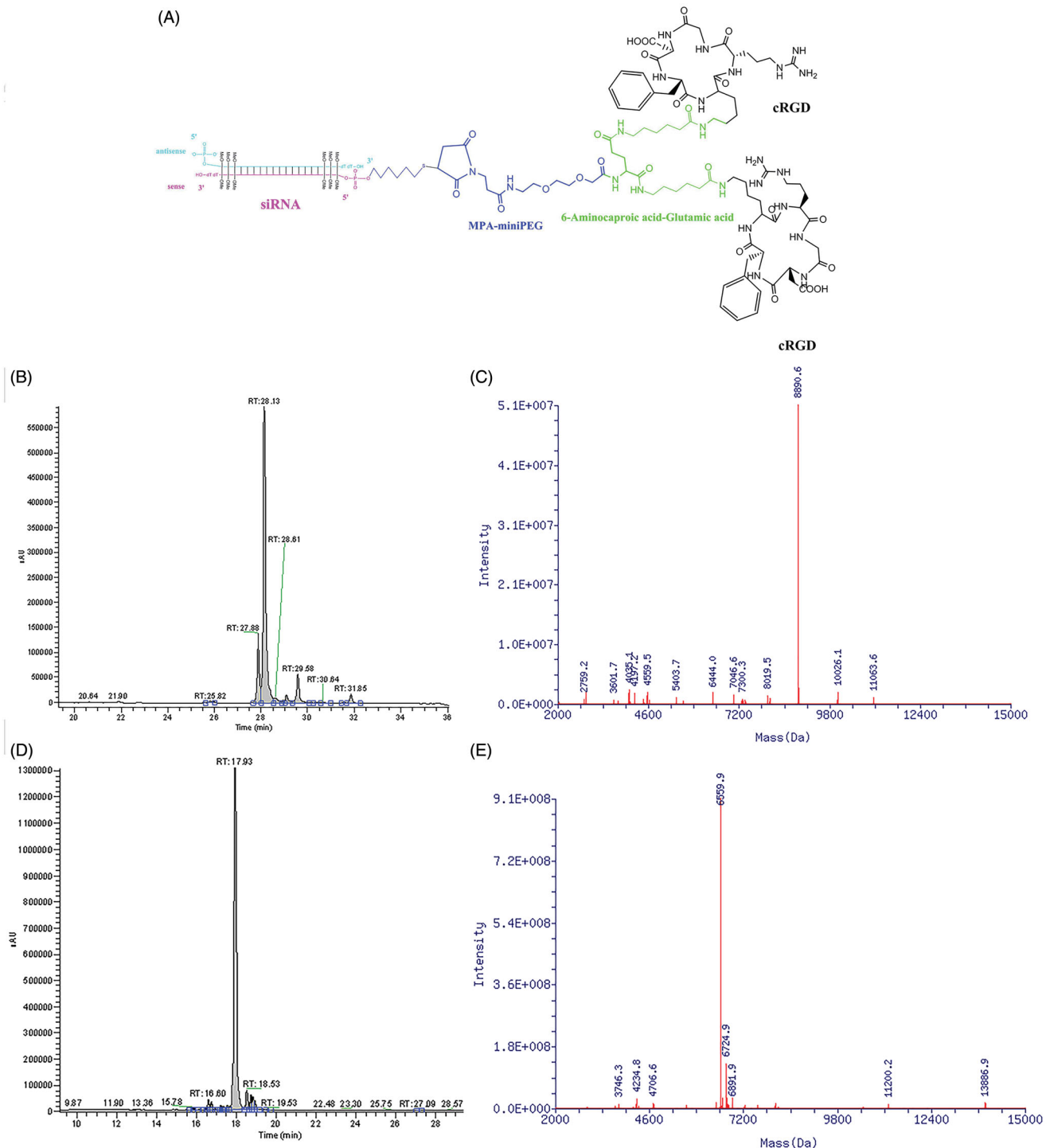


Figure 1. The schematic depiction and characterization of biRGD-siRNA. (A) The diagram of biRGD-siRNA conjugate. The [cyclo(Arg-Gly-Asp-D-Phe-Lys)-Ahx]₂-Glu-PEG-MAL (biRGD) peptide was conjugated to 5'-phosphate of sense strand of siRNA through thiol-maleimide linker. The backbone of siRNA strand was modified with 2'-O-methyl (2'-OMe) ribose in recommended nucleotides. (B, C) The high performance liquid chromatogram (HPLC) and mass spectrogram (MS) results of biRGD-conjugated sense stranded of VEGFR2 siRNA. (D, E) The high performance liquid chromatogram (HPLC) and mass spectrogram (MS) results of antisense stranded of VEGFR2 siRNA.

3.3. Anti-tumor activity of biRGD-siVEGFR2 monotherapy

As shown in Figure 3(A-D), tumor growth was recorded by bio-imaging and luciferase signal intensity was quantified and normalized, which showed that intratumoral fluorescence intensity of biRGD-siVEGFR2 (5 nmol/20 g) group was significantly lower than that of saline and biRGD-siNC

(5 nmol/20 g) groups. Tumor volume measurements further confirmed that biRGD-siVEGFR2 (5 nmol/20 g) significantly inhibited tumor growth and gefosufine did not affect its anti-tumor effect in combination therapy. Furthermore, there was no significant difference in inhibitory effect between biRGD-siVEGFR2 (5 nmol/20 g) and biRGD-siVEGFR2 (2 nmol/20 g) groups, suggesting that intravenous injection of

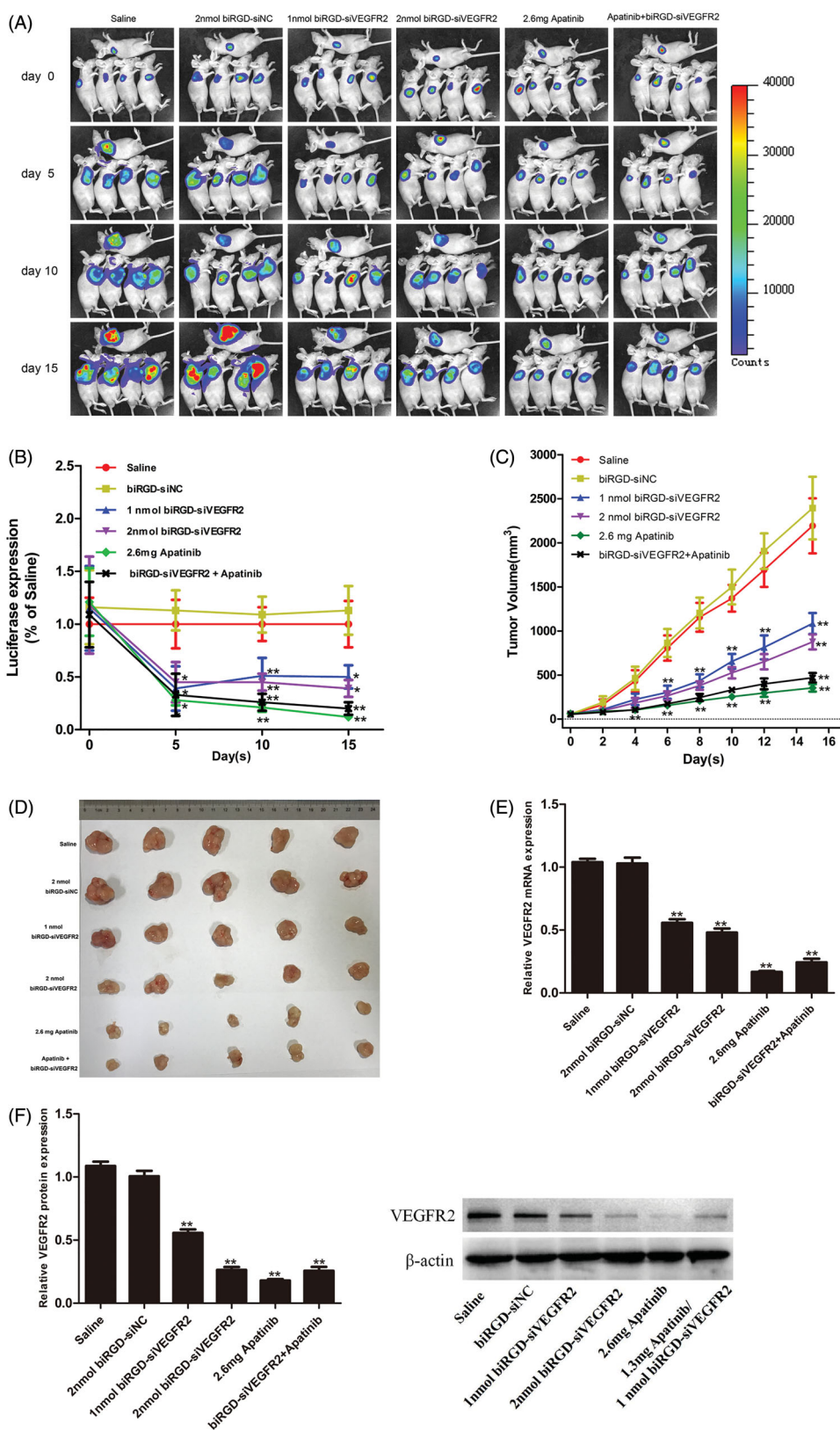


Figure 2. Anti-tumor activity and mechanism of biRGD-siVEGFR2 and its combination therapy with apatinib in NSCLC subcutaneous xenografts model. Six groups of NSCLC-bearing mice were treated as follows: Saline, biRGD-siNC (2 nmol/20 g), biRGD-siVEGFR2 (1 nmol/20 g), biRGD-siVEGFR2 (2 nmol/20 g), apatinib (2.6 mg/20 g) or biRGD-siVEGFR2 (1 nmol/20 g)+apatinib (1.3 mg/20 g). biRGD-siVEGFR2 was intravenously injected every 48 hours for seven times and apatinib was given intragastrically in the same interval. (A) IVIS bioluminescence imaging of NSCLC-bearing mice. (B) Tumor bioluminescence intensity of each group. Luminescence from tumors was measured and quantified by the IVIS imaging system. The data were normalized to saline group. (C) The tumor growth curve. Tumor volumes were measured before each treatment. (D) The image of *ex vivo* tumor from each group. Three days after the last treatment, tumors were isolated from mice and photographed. (E, F) Analysis of the expression of VEGFR2 in tumor tissues. Tumor tissues were collected to detect the expression levels of VEGFR2 mRNA and protein by RT-qPCR and western blot (normalized to β-actin level), respectively. * $P < 0.05$, ** $P < 0.01$ vs. saline group.

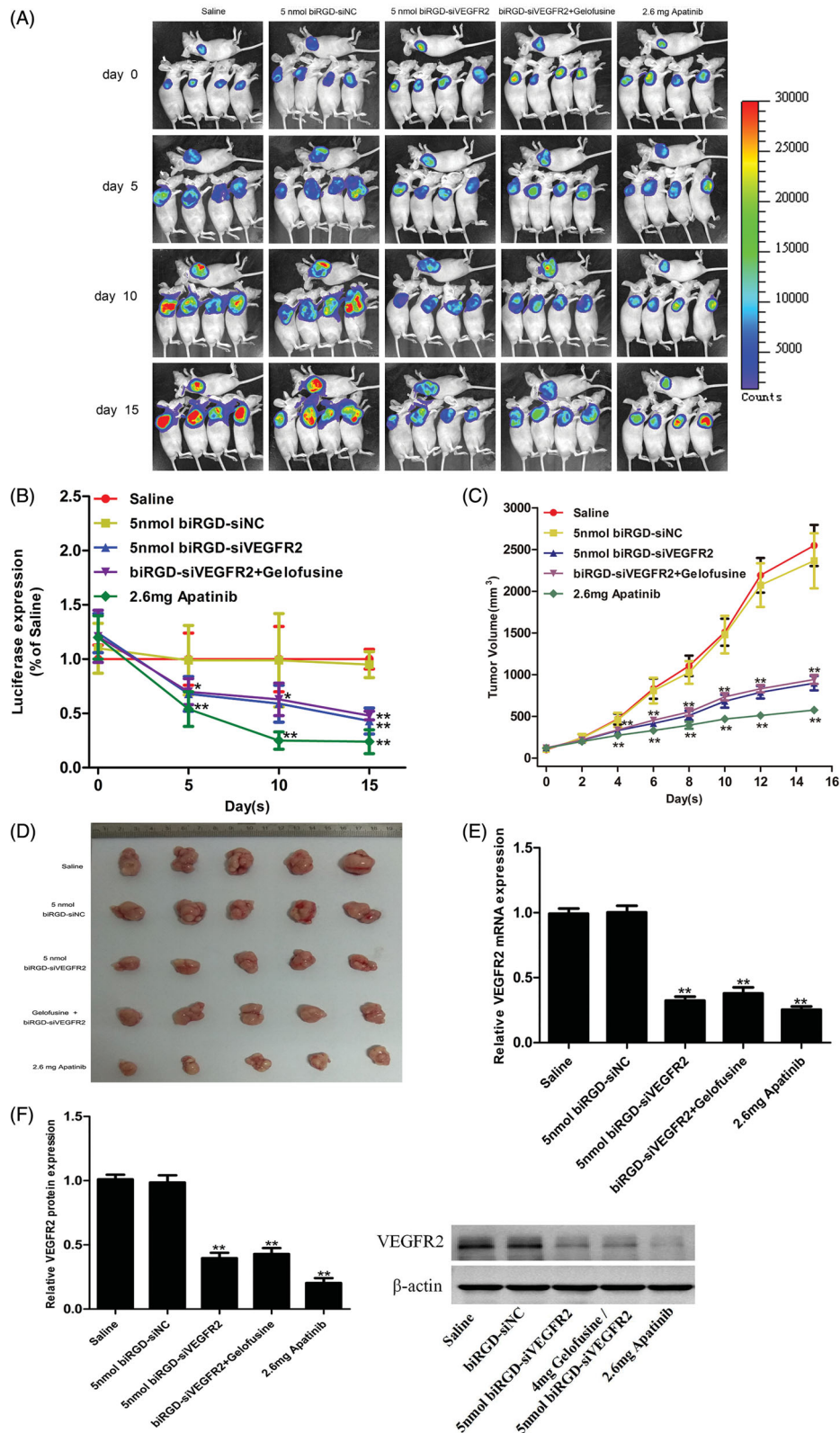


Figure 3. Anti-tumor activity of biRGD-siVEGFR2 monotherapy. Five groups of NSCLC-bearing mice were treated with saline, biRGD-siNC (5 nmol/20 g), biRGD-siVEGFR2 (5 nmol/20 g), a mixture of biRGD-siVEGFR2 (5 nmol/20 g) and gefolusine (4 mg/20 g) or apatinib (2.6 mg/20 g). biRGD-siVEGFR2 or its gefolusine mixture was injected every 48 hours for seven times and apatinib was given intragastrically in the same interval. (A) IVIS luminescent imaging of NSCLC-bearing mice. (B) Tumor bioluminescence intensity of each group. (C) The tumor growth curve. (D) The image of *ex vivo* tumor from each group. (E, F) Analysis of the expression of VEGFR2 in tumor tissues. Tumor tissues were collected to detect the expression levels of VEGFR2 mRNA and protein by RT-qPCR and western blot (normalized to β -actin level), respectively. * $P < 0.05$, ** $P < 0.01$ vs. saline group.

biRGD-siVEGFR2 at a dose of 2 nmol/20 g/48 h may be a suitable administration dose because the cellular uptake of biRGD-siVEGFR2 at this dosage might be saturated.

RT-qPCR and western blot results revealed that compared with saline group and biRGD-siNC (5 nmol/20g) group, the other treatment groups significantly inhibited the expression of VEGFR2 and gelofusine addition did not affect the silencing efficiency of biRGD-siVEGFR2 as shown in Figure 3(E,F).

3.4. Evaluation of the effects of biRGD-siVEGFR2 on angiogenesis and tumor cells proliferation via immunohistochemistry assay

Immunohistochemistry assay showed that angiogenesis density and the number of proliferating cells in tumor tissues

among all treatment groups were reduced to various extents compared with saline group and biRGD-siNC group (Figure 4(A,B)), which suggested that inhibition of tumor angiogenesis might negatively affect tumor growth via reducing supply of nutrition from blood to cancer cells.

3.5. The evaluation of liver and renal toxicity and immunogenicity of biRGD-siVEGFR2

Hematoxylin-eosin staining results indicated that co-injection of gelofusine and biRGD-siVEGFR2 could alleviate the renal toxicity caused by high-dose of biRGD-siVEGFR2. Long-term treatment with apatinib (2.6 mg/20 g) also produced significant renal toxicity, but a combination treatment of

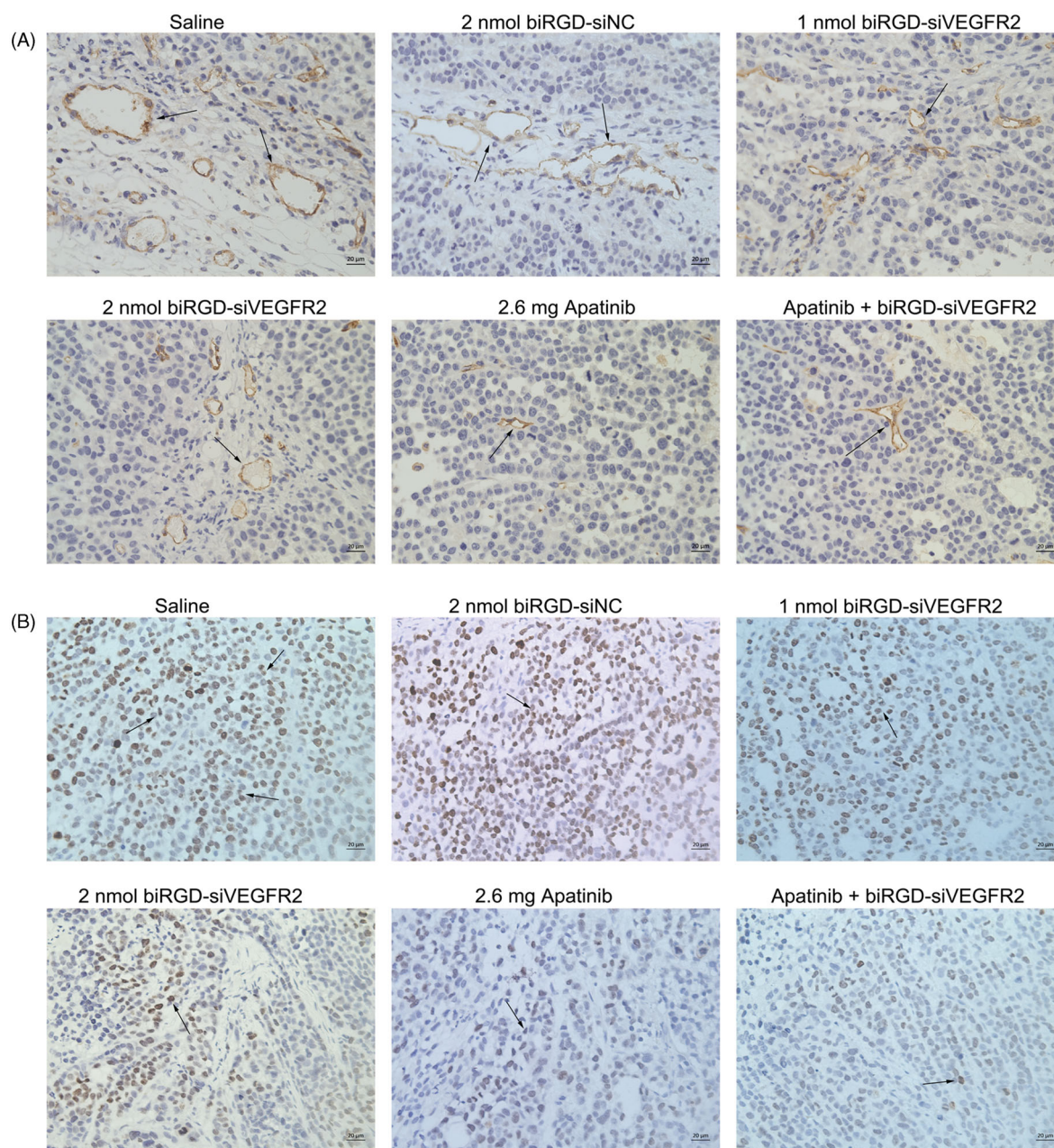


Figure 4. The effect of biRGD-siVEGFR2 on angiogenesis and tumor proliferation. (A) Immunohistochemical staining with CD31 was used to detect neovascularization in tumor tissues at $\times 400$ original magnification (indicated by arrows). (B) Immunohistochemical staining with ki67 was used to detect cell proliferation in tumor tissues at $\times 400$ original magnification (indicated by arrows). Positive cells were brown. Bar = 20 μm .

biRGD-siVEGFR2 and low-dose apatinib (1.3 mg/20 g) did not show significant renal toxicity (Figure 5(A,B)). Furthermore, we tested the concentrations of AST, ALT, Cr and BUN in the

serum of tumor-bearing nude mice after long-term administration. Compared with saline group, all biochemical parameters had no significant changes in two low-dose

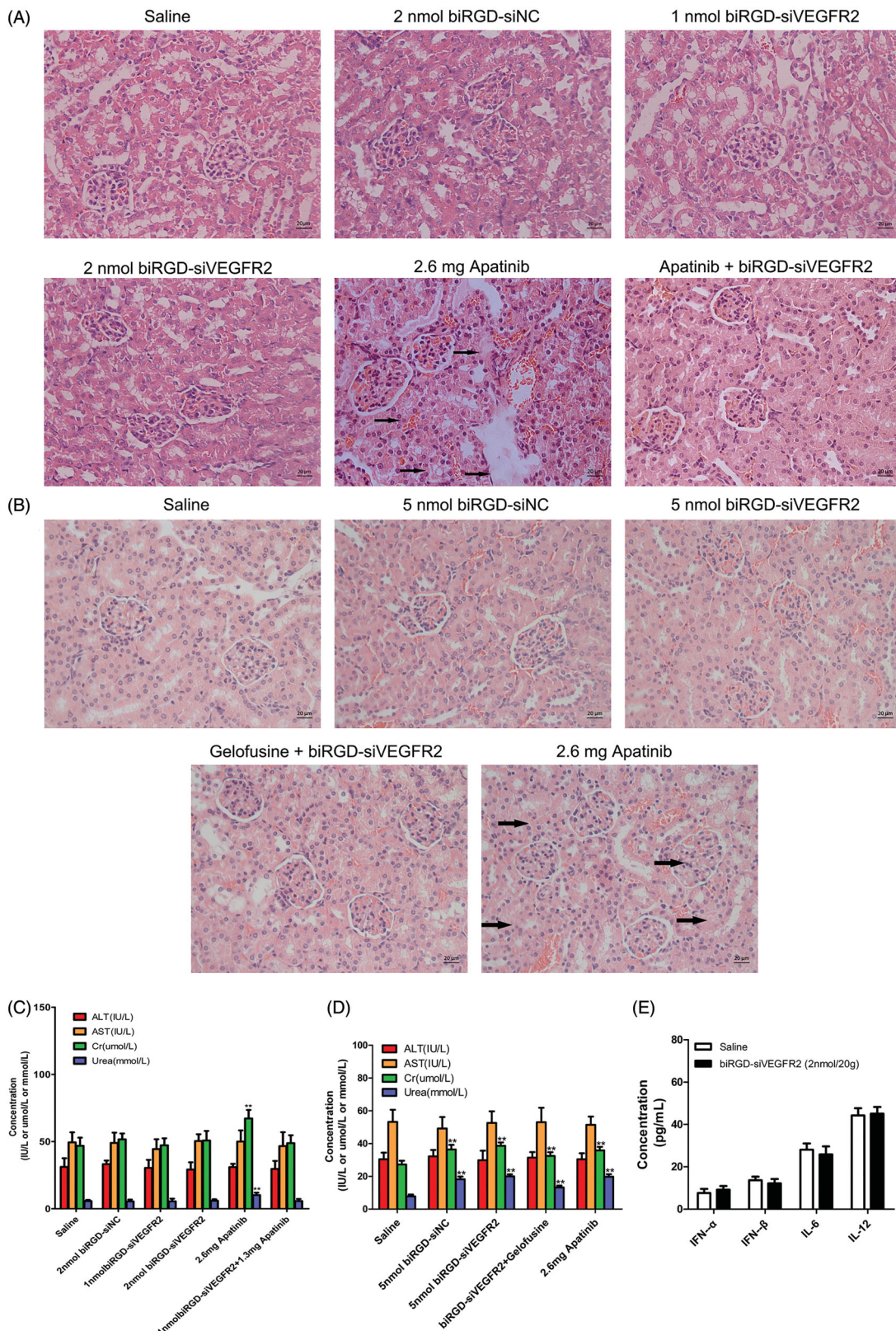


Figure 5. Toxicity and immunogenicity assessment of biRGD-siVEGFR2 *in vivo*. (A, B) Analysis of H&E stained sections of kidneys from *in vivo* anti-tumor assays. Black arrows indicate interstitial hyperemia. (C, D) Serum biochemical indicators from *in vivo* anti-tumor assays were used to assess potential liver and kidney toxicity. Three days after the last administration, blood serum was measured for AST, ALT, Cr and BUN in each group. (E) Analysis of IL-6, IL-12, IFN- β and IFN- α levels in the serum from C57BL/6J mice at six hours after the single injection of saline or biRGD-siVEGFR2 (2 nmol/20 g). ** $P < 0.01$, versus saline group, $n = 5$; bar = 20 μm .

biRGD–siVEGFR2 treatment groups. However, when the dosage of biRGD–siVEGFR2 was increased to 5 nmol/20 g, the concentrations of Cr and BUN in serum significantly increased while co-injection of gelofusine attenuated this trend. In addition, a significant increase was found in the concentrations of Cr and BUN in apatinib (2.6 mg/20 g) group, but the combination group of biRGD–siVEGFR2 (1 nmol/20g) and apatinib (1.3 mg/20 g) did not show significant changes (Figure 5(C,D)).

As shown in Figure 5(E), there were no significant differences in serum levels of IFN- α , IFN- β , IL-6 and IL-12 between the treatment group and saline group in C57BL/6J mice with intact immune system, indicating that biRGD–siVEGFR2 did not elicit an immune response. All the results suggested that biRGD–siVEGFR2 had lower toxicity and higher safety compared with apatinib.

4. Discussion

In NSCLC, tumor angiogenic pathway has been identified as important therapeutic target, which is essential in the process of primary tumor growth, proliferation and metastasis (Hall et al., 2015). Vascular endothelial growth factor receptor 2 (VEGFR2) is a transmembrane protein that is the key tyrosine kinase receptor for angiogenic signaling in NSCLC (Pajares et al., 2012). In the current clinical application, targeting tumor angiogenesis has been approached through monoclonal antibodies such as bevacizumab that blocks VEGF–VEGFR binding or small molecule TKIs such as apatinib that selectively inhibits VEGFR2 phosphorylation (Mok et al., 2014; Fan et al., 2020). As an emerging gene-targeted therapeutic technology, siRNA interference technology, which provides a new therapeutic strategy for cancer therapy due to its powerful gene silencing mechanism, has attracted widespread attention in biomedical field (Setten et al., 2019; Weng et al., 2019). In addition to small molecular inhibitors or antibody drugs, RNAi technology to inhibit VEGFR2 is also an effective method for anti-angiogenesis and tumor suppression (Liu et al., 2014a,b).

In our study, we obtained an siRNA conjugate that can silence VEGFR2 expression by linking siVEGFR2 covalently to an optimized bivalent cyclic ([cyclo(Arg-Gly-Asp-D-Phe-Lys)-Ahx]₂-Glu-PEG-MAL) peptide through the thiol-maleimide linker, which could specifically bind to integrin α v β 3 receptors overexpressing on the surface of tumor angiogenesis endothelial cells. Briefly, the specific method of siRNA conjugate synthesis was the same as our previous report (Cen et al., 2018). Our results showed that peptide–siRNA conjugates with accurate molecular weight were successfully obtained and they had no obvious immunogenicity *in vivo*. Meanwhile, our results demonstrated that biRGD–siVEGFR2 could substantially slow down NSCLC growth via inhibiting neovascularization and tumor cells proliferation.

In vivo antitumor pharmacodynamic studies in NSCLC A549 tumor xenograft model, we observed that biRGD–siVEGFR2 treatment groups significantly inhibited tumor growth in the early stage, but the inhibitory effect became weaker in the late stage of tumor development.

Moreover, there was no obvious dose-dependent in a small range of dosage we tested. The following possible reasons account for this. (1) Limited number of α v β 3 receptors on the surface of neovascular endothelial cells. As biRGD–siVEGFR2 dosage increased, α v β 3 receptors gradually reached to saturation and the additional biRGD–siVEGFR2 molecules had no extra binding sites for endocytosis. (2) Moreover, lower escape capacity of biRGD–siVEGFR2 molecules in the endosome may be the another key factor for its RNAi activity in cytoplasm, which may be overcome by increasing functional structure to promote the release of biRGD–siVEGFR2 molecules from endosome.

Taken together, we selected a powerful siVEGFR2 sequence and constructed the biRGD–siVEGFR2 conjugate. Compared with nanoparticles, the biRGD–siVEGFR2 conjugate obtained by chemical synthesis has obvious advantages such as relatively small size, good pharmacokinetics, low immunogenicity and good reproduction, all of which make it potentially suit for clinical translation.

Apatinib, a specific anti-angiogenesis inhibitor targeting VEGFR2, has shown encouraging anticancer activity in a wide range of malignancies including non-small-cell lung cancer (Zhang, 2015). Nevertheless, some side effects were observed during its clinical treatment. The most common adverse reactions were urinary protein, hypertension and hand-foot syndrome (Xue et al., 2018). In this study, we administered apatinib intragastrically with clinically regular dosage and found its tumor inhibition effect was the most pronounced among all treatment groups during the treatment. However, a significant increase in the serum concentrations of Cr and BUN was observed in apatinib-treated mice. Additionally, a small amount of necrotic epithelial cells were deposited in the renal tubules, accompanied by renal interstitial hyperemia, indicating that apatinib had certain nephrotoxicity for long-term treatment.

It is undeniable that the levels of Cr and BUN in the serum were significantly increased and the renal pathological section was abnormal when biRGD–siVEGFR2 therapeutic dosage reached 5 nmol/20 g, suggesting slight nephrotoxicity. Yet, co-injection of gelofusine relieved the toxicity caused by high-dose of biRGD–siVEGFR2. Early studies have shown that gelofusine, acting as an effective renal protective agent, can reduce the reabsorption of biRGD–siRNA, thereby alleviating kidney damage (Cen et al., 2018; Liao et al., 2018). In addition, biRGD–siVEGFR2 had no obvious liver and kidney toxicity under 2 nmol/20 g therapeutic dosage.

Interestingly, although the antitumor effect of biRGD–siVEGFR2 was not as good as that of regular dosage of apatinib, its toxicity was much lower than that of apatinib. In the meanwhile, biRGD–siVEGFR2 in combination with low-dose apatinib could achieve the same antitumor effect as the regular dosage of apatinib without obvious nephrotoxicity. These reasons may explain the phenomenon. Apatinib, an effective small molecule inhibitor, could selectively bind to tyrosine kinase of VEGFR2 and quickly inhibit the activity of VEGFR2 protein, while biRGD–siVEGFR2 could directly silence the expression of VEGFR2 via RNAi and sustain anti-tumor activity for longer time. Moreover, biRGD–siVEGFR2

could be used as an effective supplementary inhibitor for tumor cells after apatinib resistance. The data in this study showed that the combination therapy with both biRGD-siVEGFR2 and lower-dosage apatinib targeted to mRNA and protein levels respectively could quickly, persistently and effectively inhibit tumor growth and reduce the toxicity of higher-dosage apatinib.

5. Conclusions

In this study, biRGD-siVEGFR2 conjugate was successfully constructed. The *in vitro* and *in vivo* data demonstrated that biRGD-siVEGFR2 could effectively knockdown VEGFR2 expression and substantially slow down NSCLC growth. Moreover, biRGD-siVEGFR2 could enhance the antitumor effect and reduce the nephrotoxicity of apatinib. In conclusion, biRGD-siVEGFR2 can effectively inhibit NSCLC growth and may provide a new treatment strategy in combination with low-dose apatinib for clinical anti-tumor therapy.

Disclosure statement

The authors report no conflict of interest.

Funding

This work was supported by the National Natural Science Foundation of China (Grant No. 82003210 and 81773641), China Postdoctoral Science Foundation (Grant No. 2019M662870), the Natural Science Foundation of Guangdong Province, China (Grant No. 2018A030313967), Guangdong Basic and Applied Basic Research Foundation, China (2020A1515110183), the Science and Technology Program of Guangzhou, China (201604020167), and Guangzhou Key Medical Discipline Construction Project Fund.

References

- Alday-Parejo B, Stupp R, Ruegg C. (2019). Are integrins still practicable targets for anti-cancer therapy? *Cancers (Basel)* 11:978.
- Arosio D, Casagrande C. (2016). Advancement in integrin facilitated drug delivery. *Adv Drug Deliv Rev* 97:111–43.
- Barata P, Sood AK, Hong DS. (2016). RNA-targeted therapeutics in cancer clinical trials: current status and future directions. *Cancer Treat Rev* 50:35–47.
- Beer AJ, Schwaiger M. (2008). Imaging of integrin alphavbeta3 expression. *Cancer Metastasis Rev* 27:631–44.
- Bray F, Ferlay J, Soerjomataram I, et al. (2018). Global cancer statistics 2018: GLOBOCAN estimates of incidence and mortality worldwide for 36 cancers in 185 countries. *CA Cancer J Clin* 68:394–424.
- Caillaud M, El Madani M, Massaad-Massade L. (2020). Small interfering RNA from the lab discovery to patients' recovery. *J Control Release* 321:616–28.
- Carmeliet P, Jain RK. (2011). Molecular mechanisms and clinical applications of angiogenesis. *Nature* 473:298–307.
- Cen B, Liao W, Wang Z, et al. (2018). Gelofusine attenuates tubulointerstitial injury induced by cRGD-conjugated siRNA by regulating the TLR3 signaling pathway. *Mol Ther Nucleic Acids* 11:300–11.
- Cen B, Wei Y, Huang W, et al. (2018). An efficient bivalent cyclic RGD-PIK3CB siRNA conjugate for specific targeted therapy against glioblastoma in vitro and in vivo. *Mol Ther Nucleic Acids* 13:220–32.
- Chen S, Liu X, Gong W, et al. (2013). Combination therapy with VEGFR2 and EGFR siRNA enhances the antitumor effect of cisplatin in non-small cell lung cancer lung cancer xenografts. *Oncol Rep* 29:260–8.
- Debacker AJ, Voutilainen J, Catley M, et al. (2020). Delivery of oligonucleotides to the liver with GalNAc: from research to registered therapeutic drug. *Mol Ther* 28:1759–71.
- Fan Y, Zhao J, Wang Q, et al. (2020). Camrelizumab plus apatinib in extensive-stage SCLC (PASSION): a multicenter, two-stage, phase 2 trial. *J Thorac Oncol* 16:299–309.
- Hall RD, Le TM, Haggstrom DE, et al. (2015). Angiogenesis inhibition as a therapeutic strategy in non-small cell lung cancer (NSCLC). *Transl Lung Cancer Res* 4:515–23.
- He S, Cen B, Liao L, et al. (2017). A tumor-targeting cRGD-EGFR siRNA conjugate and its anti-tumor effect on glioblastoma in vitro and in vivo. *Drug Deliv* 24:471–81.
- Hu B, Zhong L, Weng Y, et al. (2020). Therapeutic siRNA: state of the art. *Sig Transduct Target Ther* 5:1–25.
- Lee SH, Kang YY, Jang HE, et al. (2016). Current preclinical small interfering RNA (siRNA)-based conjugate systems for RNA therapeutics. *Adv Drug Deliv Rev* 104:78–92.
- Liao W, Qin Y, Liao L, et al. (2018). Protective effect of gelofusine against cRGD-siRNA-induced nephrotoxicity in mice. *Ren Fail* 40:187–95.
- Liu L, Liu X, Xu Q, et al. (2014a). Self-assembled nanoparticles based on the c(RGDfK) peptide for the delivery of siRNA targeting the VEGFR2 gene for tumor therapy. *Int J Nanomedicine* 9:3509–26.
- Liu X, Wang W, Samarsky D, et al. (2014b). Tumor-targeted in vivo gene silencing via systemic delivery of cRGD-conjugated siRNA. *Nucleic Acids Res* 42:11805–17.
- Manzo A, Montanino A, Carillio G, et al. (2017). Angiogenesis inhibitors in NSCLC. *Int J Mol Sci* 18:2021.
- Mok T, Gorbunova V, Juhasz E, et al. (2014). A correlative biomarker analysis of the combination of bevacizumab and carboplatin-based chemotherapy for advanced nonsquamous non-small-cell lung cancer: results of the phase II randomized ABIGAIL study (BO21015). *J Thorac Oncol* 9:848–55.
- Ozcan G, Ozpolat B, Coleman RL, et al. (2015). Preclinical and clinical development of siRNA-based therapeutics. *Adv Drug Deliv Rev* 87:108–19.
- Pajares MJ, Agorreta J, Larrayoz M, et al. (2012). Expression of tumor-derived vascular endothelial growth factor and its receptors is associated with outcome in early squamous cell carcinoma of the lung. *J Clin Oncol* 30:1129–36.
- Piperdi B, Merla A, Perez-Soler R. (2014). Targeting angiogenesis in squamous non-small cell lung cancer. *Drugs* 74:403–13.
- Ruger J, Ioannou S, Castanotto D, et al. (2020). Oligonucleotides to the (gene) rescue: FDA approvals 2017–2019. *Trends Pharmacol Sci* 41:27–41.
- Setten RL, Rossi JJ, Han SP. (2019). The current state and future directions of RNAi-based therapeutics. *Nat Rev Drug Discov* 18:421–46.
- Shen J, Liu H, Mu C, et al. (2017). Multi-step encapsulation of chemotherapy and gene silencing agents in functionalized mesoporous silica nanoparticles. *Nanoscale* 9:5329–41.
- Shen J, Zhang W, Qi R, et al. (2018). Engineering functional inorganic-organic hybrid systems: advances in siRNA therapeutics. *Chem Soc Rev* 47:1969–95.
- Tian S, Quan H, Xie C, et al. (2011). YN968D1 is a novel and selective inhibitor of vascular endothelial growth factor receptor-2 tyrosine kinase with potent activity in vitro and in vivo. *Cancer Sci* 102:1374–80.
- Weng Y, Xiao H, Zhang J, et al. (2019). RNAi therapeutic and its innovative biotechnological evolution. *Biotechnol Adv* 37:801–25.
- Wittrup A, Lieberman J. (2015). Knocking down disease: a progress report on siRNA therapeutics. *Nat Rev Genet* 16:543–52.
- Xue JM, Astere M, Zhong MX, et al. (2018). Efficacy and safety of apatinib treatment for gastric cancer, hepatocellular carcinoma and non-small cell lung cancer: a meta-analysis. *Onco Targets Ther* 11:6119–28.
- Yang Q, Chen T, Wang S, et al. (2020). Apatinib as targeted therapy for advanced bone and soft tissue sarcoma: a dilemma of reversing multidrug resistance while suffering drug resistance itself. *Angiogenesis* 23:279–98.
- Zhang H. (2015). Apatinib for molecular targeted therapy in tumor. *Drug Des Devel Ther* 9:6075–81.